

Local immune checkpoint blockade therapy by an adenovirus encoding a novel PD-L1 inhibitory peptide inhibits the growth of colon carcinoma in immunocompetent mice

Susumu Ishiguro^{a,1}, Deepa Upreti^{a,1}, Molly Bassette^{a,b}, E.R. Azhagiya Singam^{a,c}, Ravindra Thakkar^a, Mayme Loyd^a, Makoto Inui^d, Jeffrey Comer^a, Masaaki Tamura^{a,*}

^a Departments of Anatomy and Physiology, Kansas State University College of Veterinary Medicine, Manhattan, KS 66506, USA

^b Department of Pathology, University of California, San Francisco, CA 94143, USA

^c Molecular Graphics and Computation Facility, College of Chemistry, University of California, Berkeley, CA 94720, USA

^d Departments of Pharmacology, Yamaguchi University Graduate School of Medicine, Ube, Yamaguchi 755-8505, Japan

ARTICLE INFO

Keywords:

PD-L1 inhibitory peptide secretory gene
PD-L1 inhibitory peptide
Adenovirus
Colon cancer
PD-L1 blockade therapy

ABSTRACT

A novel peptide that interferes with the PD-1/PD-L1 immune checkpoint pathway, termed PD-L1 inhibitory peptide 3 (PD-L1ip3), was computationally designed, experimentally validated for its specific binding to PD-L1, and evaluated for its antitumor effects in cell culture and in a mouse colon carcinoma syngeneic murine model. In several cell culture studies, direct treatment with PD-L1ip3, but not a similar peptide with a scrambled sequence, substantially increased death of CT26 colon carcinoma cells when co-cultured with murine CD8⁺ T cells primed by CT26 cell antigens. In a syngeneic mouse tumor model, the growth of CT26 tumor cells transduced with the PD-L1ip3 gene by an adenovirus vector was significantly slower than that of un-transduced CT26 cells in immunocompetent mice. This tumor growth attenuation was further enhanced by the coadministration of the peptide form of PD-L1ip3 (10 mg/kg/day). The current study suggests that this peptide can stimulate host antitumor immunity via blockade of the PD-1/PD-L1 pathway, thereby increasing CD8⁺ T cell-induced death of colon carcinoma cells. The tumor site-specific inhibition of PD-L1 by an adenovirus carrying the PD-L1ip3 gene, together with direct peptide treatment, may be used as a local immune checkpoint blockade therapy to inhibit colon carcinoma growth.

Introduction

In the United States, colorectal cancer (CRC) is the second leading cause of cancer-related death in both sexes combined with ~104,270 new cases and 52,980 deaths reported in 2021. Because of improvements in early detection and treatment, the current five-year survival rate is 90% in patients diagnosed with early-stage CRC. However,

survival rates of patients diagnosed with regional and distant metastases are 72% and 15%, respectively [1]. Therefore, CRC contributes to a significant portion of cancer-dependent mortality and morbidity. Accordingly, novel cancer prevention and therapeutic strategies for both primary and metastatic CRC are urgently needed.

Given that current strategies for CRC treatment have limited success, immune checkpoint blockade therapy (ICBT) has emerged as a powerful

Abbreviations: PD-1, Programmed death-1; PD-L1, Programmed death-ligand-1; PD-L1ip3, PD-L1 inhibitory peptide 3; PD-L1ip3SC, Scrambled analogue of PD-L1ip3; ICBT, Immune checkpoint blockade therapy; CRC, Colorectal cancer; MSI, Microsatellite instability; dMMR, DNA mismatch repair gene defects; ICI: Immune checkpoint inhibitor; RPMI, Roswell Park Memorial Institute; FBS, Fetal bovine serum; MEM, Eagle's minimum essential medium; PBS, Phosphate-buffered saline; MM-PBSA, Molecular mechanics-Poisson-Boltzmann and surface area; NAMD, Nanoscale molecular dynamics; PD-L1ip gene encoding adenovirus vector, Ad-PD-L1ip; MD, Molecular dynamics; RT-qPCR, Reverse transcription quantitative polymerase chain reaction; MOI, Multiplicity of infection; MTT, 3-(4,5-dimethylthiazol-2-yl)-2,5-diphenyltetrazolium bromide; SQ, Subcutaneous.

* Corresponding author.

E-mail addresses: isusumu@vet.ksu.edu (S. Ishiguro), deepa07@vet.ksu.edu (D. Upreti), Molly.Bassette@ucsf.edu (M. Bassette), eazhagi@berkeley.edu (E.R.A. Singam), ravithakkar@vet.ksu.edu (R. Thakkar), mkloyd@ksu.edu (M. Loyd), minui@yamaguchi-u.ac.jp (M. Inui), jeffcomer@ksu.edu (J. Comer), mtamura@vet.ksu.edu (M. Tamura).

¹ These authors contributed equally to this work.

<https://doi.org/10.1016/j.tranon.2021.101337>

Received 24 November 2021; Received in revised form 18 December 2021; Accepted 21 December 2021

1936-5233/© 2022 Published by Elsevier Inc. This is an open access article under the CC BY-NC-ND license (<http://creativecommons.org/licenses/by-nc-nd/4.0/>).

new tool for cancer therapy. However, only CRCs associated with microsatellite instability (MSI) or DNA mismatch repair gene defects (dMMR, ~15% of all CRCs [2]) are sensitive to this therapy [3,4] and systemic side effects remain major concerns [4–6]. This poor sensitivity to ICBT is either due to poor tumor infiltration of functional T cells or T cell exhaustion [7]. Combination treatment with an oncolytic virus and an immune checkpoint inhibitor (ICI) has been reported to be very effective in increasing therapeutic efficacy [8] and tumor immunogenicity since the oncolytic virus infection exposes neoantigens, thus causing additional T cell infiltration into the tumor tissue [8,9]. However, an oncolytic virus is a pathogen and its systemic administration induces a robust host immune response against the virus and causes unwanted side effects [10].

Accordingly, local immune checkpoint inhibition coupled with some oncolysis may be an ideal ICBT. The protein programmed cell death-1 ligand (PD-L1) is significantly upregulated by cancer cells [11]. PD-L1 stimulates the immune checkpoint mechanism by interacting with PD-1 molecules expressed on T cells, attenuating cytotoxic T cell-dependent oncolysis [12]. Current immunotherapies targeting the PD-1/PD-L1 pathway rely on systemic inhibition of PD-L1 or PD-1, resulting in immune-related adverse events in 12%–37% of patients treated, some of which are life-threatening [13]. Hence, a more local blockade of PD-L1, restricted to cancer tissue, would be desirable, with less potential for off-target effects. Therefore, studying the PD-L1-targeted immune checkpoint blockade along with mild oncolysis in cancer tissue as a local ICBT becomes imperative. Here, we report on the design of a novel peptide that specifically binds PD-L1; our results demonstrate that a combination treatment of an adenovirus vector encoding a secretory gene for this peptide along with direct administration of the peptide itself inhibits the growth of murine colon carcinoma cells in cell culture and a syngeneic murine model *via* stimulation of cytotoxic T cell function.

Materials and methods

Animals

Female BALB/c mice were obtained from Charles River Laboratories International, Inc. and housed in a clean facility under controlled conditions of temperature (20–26 °C), with 30%–70% relative humidity and light (12:12 h light-dark cycles). All mice were held for a week to acclimatize before the treatment and were housed humanely according to university, state, and federal guidelines (AAALAC) in the AAALAC-accredited animal resource facilities of the Kansas State University College of Veterinary Medicine. The mice were observed daily, and body weights were obtained on alternate days. All animal experiments adhered strictly to protocols approved by the Kansas State University Institutional Animal Care and Use Committee (Protocol # 4393) and Institutional Biosafety Committee (Protocol # 1317).

Materials

The mouse colon carcinoma cell line CT26.CL25 (CRL-2639) and mouse immature dendritic cell line JAWSII (CRL-11,904) were purchased from American Type Culture Collection (ATCC, Manassas, VA). RPMI 1640 was obtained from Mediatech, Inc. (Manassas, VA). Fetal bovine serum (FBS) was procured from Biowest (Riverside, MO). Penicillin-streptomycin stock was obtained from Lonza Rockland, Inc. (Allendale, NJ). Thermo Fisher Scientific (Waltham, MA) supplied the 200 mM sodium pyruvate, MEM non-essential amino acids (100×), MEM amino acids (100×), 200 mM L-glutamine, antibiotic-antimycotic (50×) (all are Gibco®). Further, 2-mercaptoethanol was purchased from Sigma-Aldrich (St. Louis, MO). Anti-cleaved Caspase-3 antibody (Asp175) was supplied by Cell Signaling Technology, Inc. (Danvers, MA).

Design of PD-L1 inhibitory peptide

To generate candidate PD-L1 binding peptides, the PinaColada program [14] was applied to an x-ray structure of human PD-1 bound to human PD-L1 (PDB ID: 4ZQK) [15]. We selected 14 candidate sequences from the output of the algorithm, which were each docked into PD-L1 near the PD-L1:PD-1 binding interface using the CABS-dock server [16] for flexible protein-peptide docking. Six docked complexes were obtained for each sequence, which were placed in a box of explicit water with dimensions of (69 Å)³. The docked complexes were then simulated for 10 ns in explicit solvent molecular dynamics using the program Amber16 [17]. We equilibrated the solvated complex by carrying out an energy minimization of 1,000 steps, 50 ps of heating, and 50 ps of density equilibration with weak restraints on the complex followed by 500 ps of constant pressure equilibration at 300 K temperature. All simulations were run with the SHAKE algorithm applied to hydrogen atoms, a 2 fs time step, and Langevin dynamics for temperature control. We estimated binding free energies by the MM-PBSA method (molecular mechanics, Poisson-Boltzmann, and surface area) [18], as implemented in Amber16. Table 1 shows the MM-PBSA estimates of the binding free energies for the 14 sequences. The root-mean-square deviations of the positions of the peptide atoms from the docked structures are given in Fig. S1. All molecular dynamics simulations used the Amber ff12SB force field [19], a timestep of 2 fs, the particle-mesh Ewald method for full electrostatics [20], and a cutoff of 9 Å for explicit non-bonded interactions. The temperature was maintained at 300 K using a Langevin thermostat and 1 atm pressure was maintained using the Monte Carlo barostat (Amber16) or Langevin piston barostat (NAMD) [21]. Long simulations of the peptides in contact with PD-L1 were performed using NAMD 2.12 [22].

Bio-layer interferometry

The binding of the computationally designed PD-L1ip3 peptide to PD-L1 was verified using a FortéBio BLItz machine (Freemont, CA). The PD-L1ip3 peptide and its scrambled analog were synthesized by GenScript (Piscataway, NJ) with no modifications or labels. Biotinylated human PD-L1 and untagged PD-1 (a positive control) were purchased from R&D Systems (Minneapolis, Minnesota). For each experiment, the BLItz machine was fitted with a fresh streptavidin biosensor tip (FortéBio). All tips were solvated in PBS buffer for 15–30 min prior to the experiments. The peptide was solvated at a concentration of ~1 mg/ml. The precise concentration of this stock solution (0.922 mg/ml) was obtained using the Pierce BCA Protein Assay Kit (Thermo Fisher Scientific) and multiple dilutions were made (corresponding to 514, 171, 17.1, 8.54, and 1.71 μM). A solution of biotinylated PD-L1 was applied to the biosensor tip during the loading phase of each experiment. PBS buffer (1×) was used for the baseline. The scrambled-sequence peptide,

Table 1

Estimated binding free energies (in kcal/mol) for peptides binding to PD-L1 calculated by MM-PBSA.

Sequence	$\Delta G_{\text{MM-PBSA}}$ (kcal/mol)
AISLHPKAKILEWPGA	-47.5
PLDIRDRVHVEKSAAS (PD-L1ip4)	-56.5
SVAVNPTPTLMDAPGG	-30.9
SVAVNDTPTLMDAAAG	-32.5
FHTLEPSLLAINTPGV	-31.4
FHTIEDSLAINTAAV	-31.9
FHTVEPSLLAINTPGV	-32.5
GTRLKPLIICVQWPGL (PD-L1ip3)	-58.7
GTRIKDLIICVQSAAL	-53.6
GTRVKPLIICVQAPGL	-43.5
LIELHPAARITWPGA	-44.7
LLEIRDVAVRVTKSAAS	-38.5
VISLHDKAAIHEWPGA	-46.1
VLDIRPRVAHVHKSAAA	-39.6

PD-L1ip3SC, served as the negative control, and PD-1, the natural binding partner of PD-L1, was a positive control.

Preparation of adenovirus vector

To generate an adenovirus expression vector encoding a gene for secreting PD-L1ip, an adenovirus expression plasmid was constructed using the pENTR/D-TOPO plasmid (the entry vector) and the Gateway-based pAd/CMV/V5-DEST vector (the destination vector) (Invitrogen Corp, Carlsbad, CA). The DNA sequence encoding an N-terminal secretion signal from the V-J2-C region of the mouse Ig kappa-chain, a short linker (AAQPARRA), a c-Myc tag (EQKLISEED), and the PD-L1ip3 sequence (GTRLKPLIICVQWPGL) or its scrambled version (VLI-KIPWLRPLPGCGTQ) was synthesized and was cloned into the entry vector. The inserts were then transferred from the entry vector into the destination vector by the LR recombination reaction according to the manufacturer's instructions. The destination vectors thus obtained were digested by Pac I and were transfected into 293A cells to produce crude adenoviral vector stocks. The adenovirus vectors were amplified by infecting 293A cells. DNA sequence analysis of adenovirus vectors for PD-L1ip3 (Ad-PD-L1ip3) and the scrambled version (Ad-PD-L1ip3SC) revealed the accuracy of the sequences of the inserts. Since Ad-PD-L1ip3 produces a larger size peptide than the original peptide form of PD-L1ip3 due to the linker and c-Myc tag sequences (AAQPARRA-EQKLISEED-GTRLKPLIICVQWPGL), additional MD simulations were performed to verify whether the complete secreted peptide constructs also led to stable complexes. A slightly greater affinity was predicted when the linker and the c-Myc tag were included. PD-L1ip3 gene expression in Ad-PD-L1ip3 transduced CT26 cells (Fig. S2) was confirmed by quantitative reverse transcription PCR (RT-qPCR), as previously described [23], using a primer pair with the forward primer 5'-TATCAGCGAGGAGGACGGTA-3' and reverse primer 5'-CAGATGATCAGGGGCTTCAG-3'. Briefly, CT26 cells were seeded into a 6-well plate (5×10^4 cells per well). After 24 h, the cells were transduced (foreign DNA introduced into another cell via a viral vector) with 50 MOI of Ad-PD-L1ip3. Total RNA was purified by TRIzol Reagent (Thermo Fisher Scientific), according to manufacturer instructions on days 3, 5, and 7 after transduction. The cells were sub-cultured twice at Days 3 and 5 using only half of the cell number at a time.

Cell culture

The CT26 murine colon carcinoma cells were cultured in RPMI 1640 supplemented with 10% v/v FBS and 1% v/v penicillin-streptomycin. Murine CD8⁺ T cells were cultured in RPMI 1640 supplemented with 1 mM sodium pyruvate, 1x MEM non-essential amino acids, 1x MEM amino acids, 1 mM L-glutamine, 1x antibiotic-antimycotic, and 0.36 mM 2-mercaptoethanol. Thereafter, these cells were cultured at 37 °C in a humidified air atmosphere containing 5% CO₂. The cell line was authenticated by short tandem repeat (STR) DNA profiling and maintained in low passage (< 15) for the present study.

Evaluation of the effect of PD-L1ip3 peptide or gene transduction by Ad-PD-L1ip3 on murine colon carcinoma cells in cell culture

The CT26 murine colon carcinoma cells (1,000 cells/well) were seeded into a 96-well plate. After 24 h, these cells were treated directly with PD-L1ip3 in peptide form (0.1–10 µg/ml) or indirectly with the PD-L1ip3 gene by Ad-PD-L1ip3 transduction (10, 20, and 50 MOI). The cells' growth was evaluated by MTT assay 24–72 h after the treatments, as described previously [24].

Evaluation of the effect of PD-L1ip3 peptide or gene transduction by Ad-PD-L1ip3 on T cell-induced death of murine colon carcinoma cells in co-culture with antigen-primed T cells

Generation of CT26 cell antigen-specific CD8⁺ T cells in vivo

First, the mice were subcutaneously (SQ) injected with CT26 cell lysate (0.5×10^6 cells/mouse in 100 µl PBS) at Day 0. JAWS II immature dendritic cells and CT26 cells previously irradiated with an X-ray dose of 100 Gy were cocultured at a 1:1 ratio for 48 h with additional treatment of LPS (1 µg/ml). The cells (0.5×10^6 cells/mouse in 200 µl PBS) were collected and administered IV via tail vein to the mice on Day 7. On Day 21, the splenocytes were harvested; the CT26 antigen-specific CD8⁺ T cells were labeled using MojoSort™ Mouse CD8 T Cell Isolation Kit (Biolegend, San Diego, CA); isolated using magnetic beads-based separation protocol with MACS® Column (Miltenyi Biotec, Bergisch Gladbach, Germany), according to the manufacturer's instructions.

Evaluation of T cell-induced death of colon carcinoma cells in co-culture

Permanently green fluorescent protein (GFP)-expressing CT26 cells (GFP-CT26) produced by GFP-lentivirus vector transduction were seeded into 12 well-plate (1×10^4 cells/well) in the presence of murine interferon-gamma (mIFNγ) at 25 ng/ml for 24 h. The cells were treated directly by PD-L1ip3 peptide (10 µM) or indirectly by Ad-PD-L1ip3 transduction (100 MOI) treated 30 min and 24 h prior to coculturing with CD8⁺ T cells (1:16 ratio), respectively. The effect of PD-L1ip3 in peptide form or gene transduction by Ad-PD-L1ip3 on CT26 cell death was analyzed by flow cytometry using LIVE/DEAD™ Fixable Violet Dead Cell Stain Kit (Invitrogen Corp). The specific death of GFP-CT26 cells was identified by GFP⁺ LIVE/DEAD⁺ gating. The Ultra-LEAF™ Purified anti-mouse CD274 (B7-H1, PD-L1) antibody (0.5 µg/ml; BioLegend) was used as a positive control of interruption of PD-1/PD-L1 interaction. PBS, PD-L1ip3SC peptide, and Ad-PD-L1ip3SC were used as negative controls.

Evaluation of Ad-PD-L1ip3 treatment and cotreatment with PD-L1ip3 peptide on colon carcinoma tumor growth in a subcutaneous syngeneic murine tumor model

The anti-tumor effect of Ad-PD-L1ip3 and PD-L1ip3 in peptide form was evaluated in BALB/c mice using a CT26 murine colon carcinoma syngeneic mouse model. The CT26 cells were transduced with 100 MOI of Ad-PD-L1ip3 or Ad-PD-L1ip3SC. At 24 h after transduction, the cells were suspended into 0.6% agarose dissolved in RPMI 1640. After filling the agarose-cell mixture into a 1 ml syringe equipped with a 27 G needle, it was solidified on ice. Mice were anesthetized with isoflurane and injected subcutaneously into the back with 5×10^5 CT26 cells in a 50 µl cell-agarose mixture. The intraperitoneal administration of PD-L1ip3 peptide (10 mg/kg) was carried out at 1 week after CT26 inoculation for 13 days (every day, 1 injection, total 13 injections). The PBS control was injected intraperitoneally with the same schedule. For the pre-immunization study, CT26 lysate (1×10^6 cells/100 µl PBS) were injected subcutaneously, 3 times with a 1-week interval. The CT26 lysate was made by subjecting the cells to 3 freeze-thaw cycles using liquid nitrogen. The mouse body weights were monitored at 2-day intervals. All mice were sacrificed 19 days after CT26 inoculation by cervical dislocation after exposure to saturated CO₂. The tumor size was measured by caliper every 2 days and the volume was calculated using the formula $0.5 \times (\text{short diameter})^2 \times (\text{long diameter})$ [25]. The tumors were weighed and fixed in 10% formalin for histological analysis.

Gene expression of PD-L1ip3 in the tumor was confirmed 2, 3, and 4 weeks after cancer cell inoculation (Fig. S3). About 20 mg of tumor tissues were used for the purification of total RNA. RNA extraction and RT-qPCR were performed as aforementioned.

Analysis of Ad-PD-L1ip3 treatment-associated apoptosis of CT26 cell tumors by immunohistochemistry

The paraffin-embedded tumor tissues were sectioned and immunostained with anti-cleaved caspase-3 antibodies. The average number of cleaved caspase-3 positive cells in five random fields ($n = 5-6$) was calculated.

Statistical analysis

All values are expressed as the mean \pm standard deviation of the mean. For all *in vitro* and *in vivo* experiments, statistical significance was evaluated using an unpaired *t*-test or ANOVA followed by Tukey's test. All experiments were conducted with multiple sample determinations with several samples ($n = 3-6$). Statistical significance was set at *, $P < 0.05$.

Results

Computational evaluation of the interaction of PD-L1 inhibitory peptide and PD-L1

Using estimates of binding free energy by the MM-PBSA method, two sequences (referred to as PD-L1ip3 and PD-L1ip4, see Table 1) were

selected, and long explicit-solvent molecular dynamics simulations of six distinct docked poses of each peptide bound to human PD-L1 were performed for the validation of complex stability. We found that PD-L1ip3 remained stably bound to PD-L1 in all six cases for at least 800 ns, while PD-L1ip4 diffused away from its putative binding site within 300 ns simulation. Fig. 1A demonstrates the conformation of the complex between PD-L1ip3 and PD-L1 with the strongest predicted binding affinity. Putative interactions between PD-L1ip3 and PD-L1 in this conformation are diagrammed in Fig. 1B. The complex appeared to be stabilized by a salt bridge between the N-terminus of the peptide and Glu58 of PD-L1, Arg3 of the peptide and Asp73, and the C-terminus of the peptide and Arg113 and Arg125. Hydrophobic contacts were noted between Lys7 and Ile8 of the peptide and Ile116 and Ala121 of PD-L1. Most of the residues of PD-L1 involved in these interactions form part of the binding interface between PD-L1 and PD-1 [15], suggesting the role of this peptide in competing with PD-1 for the PD-L1 binding site. This computational analysis was performed with human PD-L1 (the only experimentally derived PD-L1 structure available) at variance with the experiments, which involved murine cells; however, most of the binding site residues are identical between humans and mice, including all residues whose side chains contact with the peptide, as shown in Fig. 1B. The only exception is that Arg113 is being replaced with Cys113 in mice; however, Arg125 is present in both cases so a salt bridge with the C-terminus can exist regardless. Notably, the affinity of murine PD-1 for

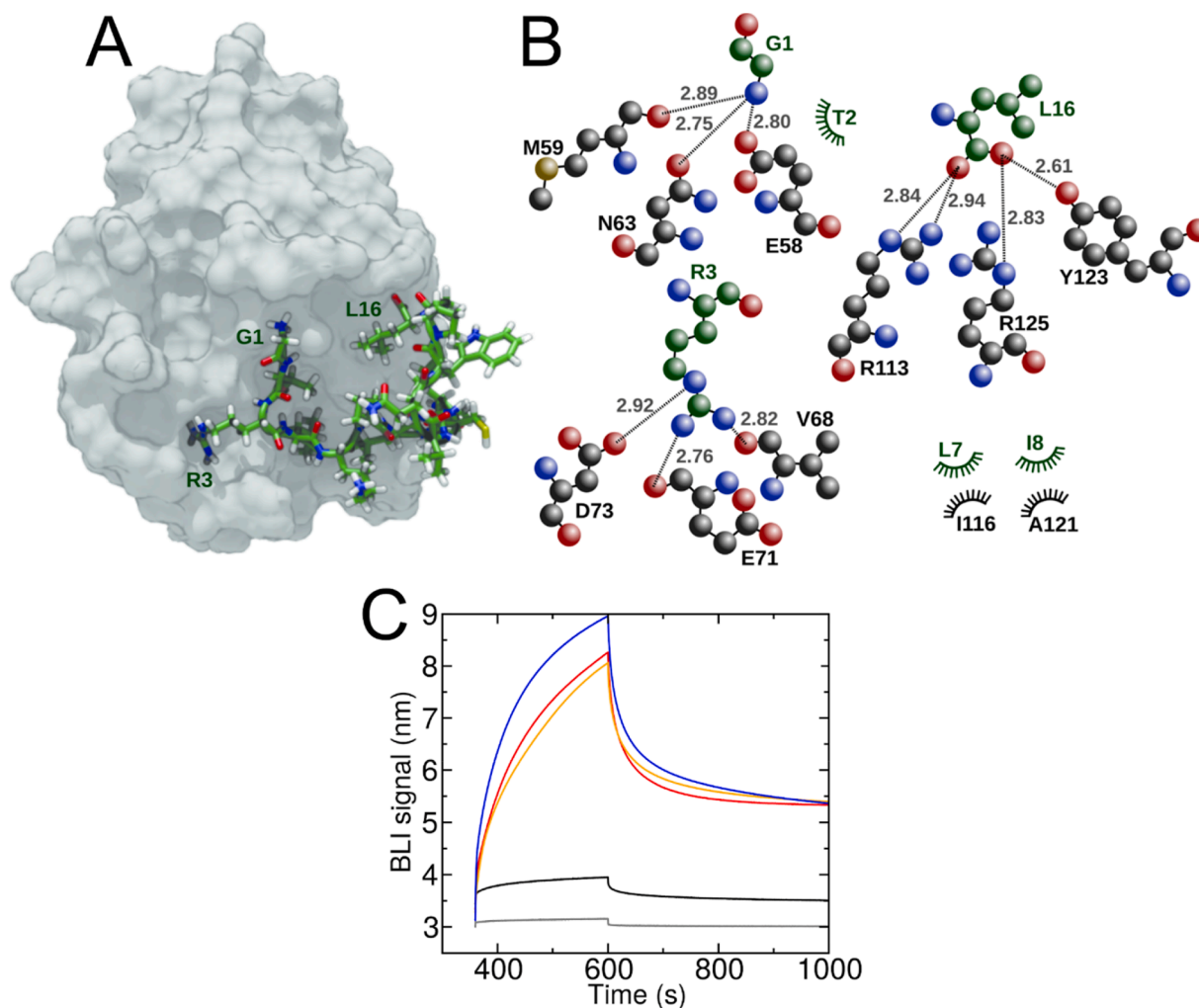


Fig. 1. Binding of newly discovered peptide PD-L1ip3 to PD-L1. (A) Predicted lowest free energy binding conformation. (B) Atomic interactions between PD-L1ip3 and PD-L1 that stabilize binding in this conformation. Carbon atoms of PD-L1ip3 are shown in green, while those of PD-L1 are shown in gray. (C) Kinetics of binding between the designed peptide (PD-L1ip3) and PD-L1 during the association and dissociation phases of bio-layer interferometry experiments for different concentrations of PD-L1ip3. Gray, black, red, orange, and blue lines correspond to PD-L1ip3 concentrations of 0, 1.71, 8.54, 17.1, and 171 μM , respectively.

human PD-L1 shows similarity to that of human PD-1 for human PD-L1 [26].

Experimental confirmation of association between the designed peptide and PD-L1

We experimentally verified that the computationally designed peptide, PD-L1ip3, exhibits specific binding to PD-L1. The peptide was synthesized commercially and the dissociation constant was determined by biolayer interferometry. PD-L1ip3 showed binding to PD-L1 with a dissociation constant of $K_D = 33 \pm 3 \mu\text{M}$ (Fig. 1C), which is only a few times weaker than the binding of PD-L1 to its natural partner PD-1 ($K_D \approx 8 \mu\text{M}$) [27]. Hence, the binding affinity of this peptide may explain the biological activity of PD-L1ip3 observed in the experiments described in the following sections. The bio-layer interferometry experiments included the scrambled version of the peptide (PD-L1ip3SC) as a negative control, which exhibited very weak binding ($K_D \approx 50 \text{ mM}$), demonstrating that PD-L1ip3 binding to PD-L1 is not merely a non-specific association.

Treatment with PD-L1ip3 peptide or transduction of the PD-L1ip3 gene did not alter the growth of colon carcinoma cells in the absence of T cells

To evaluate therapeutic potential and cytotoxicity of the PD-L1ip3 peptide and gene transduction by Ad-PD-L1ip3, cell viability of CT26 cells was analyzed using MTT assay in the presence of mIFN γ (25 ng/ml), which was used to increase PD-L1 expression in cancer cells [28]. The scrambled sequence version of PD-L1ip3 (PD-L1ip3SC) and the adenovirus carrying the corresponding scrambled sequence gene (Ad-PD-L1ip3SC) were used as negative controls. As shown in Fig. S4, neither treatment with the peptide form of PD-L1ip3 (0.1–10 $\mu\text{g/ml}$), nor the control peptide PD-L1ip3SC, nor gene expression by the Ad-PD-L1ip3 or Ad-PD-L1ip3SC gene (10–50 MOI) altered the cell viability of CT26 cells regardless of the pretreatment with mIFN γ . Although a slight decrease of cell viability was observed at 72 h after the treatment with 10 $\mu\text{g/ml}$ PD-L1ip3SC, this decrease was not significantly different in comparison to PBS. These results indicate that both PD-L1ip3 peptide and its gene expression by adenovirus vector in cancer cells do not alter the cell viability and may have no inherent cytotoxicity for cancer cells in the absence of T cells.

Treatment with PD-L1ip3 peptide or transduction of the PD-L1ip3 gene significantly increased T cell-induced death of CT26 murine colon carcinoma cells

To analyze the effect of administration of PD-L1ip3 in peptide form and gene transduction by Ad-PD-L1ip3 on T cell function and cancer cell death, CT26 cell antigen-primed T cells (CT26-T cells) were generated by treatment of mice with CT26 cell lysate and irradiated CT26 cells, as described in the Methods. Preparation of the splenocytes and subsequent isolation of the CD8 $^+$ T cells were carried out on the same day of the co-culture study. Cell death was analyzed by flow cytometry using live/dead staining dye. First, the most appropriate ratio of cancer cells to T cells was determined by varying their ratio from 1:4 to 1:24 (CT26 cells: T cells) in co-culture. Fig. 2A shows that death of CT26 cells was induced by antigen-primed T cells even within 24 h after beginning co-culture when the number of T cells was at least 12 times greater than the number of CT26 cells. The antigen-primed T cells induced death of CT26 cells to a greater extent than naïve T cells 24 h after incubation; however, this difference is less conspicuous for longer times. At 48 h, the effect of antigen-primed and naïve T cells appears similar. Death of CT26 cells significantly declined 72 h after incubation in all tested ratios. Based on these experiments, a cancer cell to T cell ratio of 1:16 was used for all following experiments.

Treatment with 10 μM of PD-L1ip3 in peptide form markedly increased the cell death of CT26 cells as compared to the PBS-treated

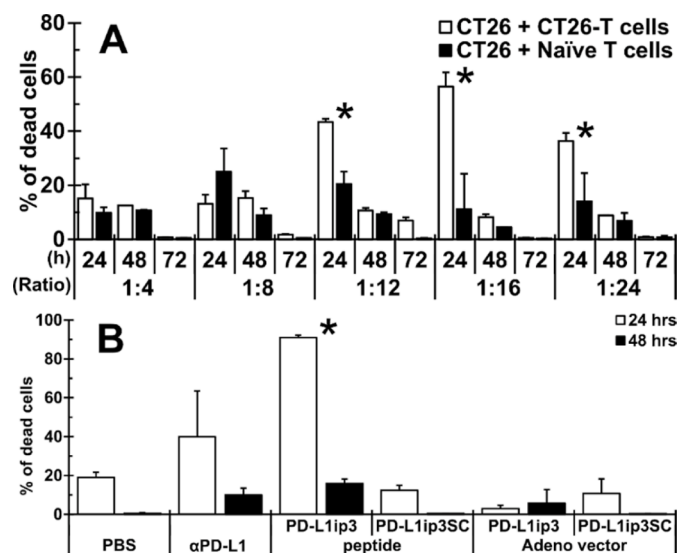


Fig. 2. Treatment with PD-L1ip3 in peptide form significantly increased T cell-induced death of CT26 cells. (A) The most effective CT26 cell antigen-primed T cell (CT26-T cell) induced death in co-cultured CT26 cancer cells, as determined by varying the ratio of CT26 cells to these antigen-primed T cells (1:4 – 1:24). The two types of cells were co-cultured for 24–72 h. The death of CT26 cells was determined by flow cytometry. Results are presented as mean \pm SD ($n = 2$). *; $P < 0.05$ with 1:4 ratio group at same time point. (B) The effect of treatment with PD-L1ip3 in peptide form and transduction of Ad-PD-L1ip3 on the death of CT26 cells induced by antigen-primed T cells. CT26 cells treated with PD-L1ip3 in peptide form (10 μM) or transduced by Ad-PD-L1ip3 (100 MOI) were cocultured with antigen-primed T cells at a 1:16 ratio. Cell death of CT26 was evaluated in the same way as in (A). Anti-PD-L1 antibody ($\alpha\text{PD-L1}$; 0.5 $\mu\text{g/ml}$) was used as a positive control. Results are presented as mean \pm SD ($n = 2$). *; $P < 0.05$ with PBS group at the same time point.

group; however, gene transduction by Ad-PD-L1ip3 into CT26 cells and subsequent co-culture with the antigen-primed T cell increased cell death of CT26 cells only to a small extent as compared to the direct peptide treatment at 72 h after the co-culture (Fig. 2B). These results indicate that treatment with PD-L1ip3 in peptide form specifically stimulates the killing of cancer cells by cancer cell antigen-primed T cells. However, the effect of gene transduction by Ad-PD-L1ip3 into CT26 cells in T cell-induced cell death in co-cultured CT26 cells is smaller than the peptide treatment and appears to require time.

Gene transduction by Ad-PD-L1ip3 and combination treatment with PD-L1ip3 peptide attenuated the growth of CT26 murine colon tumors in mice

To evaluate the effect of PD-L1ip3 *in vivo*, we transduced the PD-L1ip3 gene into CT26 cells using a dosage of 100 MOI of Ad-PD-L1ip3. The cells were inoculated subcutaneously (SQ) in the back of the mice. In the first trial as shown in Fig. 3, Ad-PD-L1ip3 transduction into CT26 cells weakly attenuated the growth of SQ tumors (average tumor volume of $848.5 \pm 400.0 \text{ mm}^3$, n.s.) and the effect was enhanced by combining this treatment with direct daily treatment with PD-L1ip3 in peptide form (10 mg/kg/day) ($533.1 \pm 143.6 \text{ mm}^3$, n.s.). By comparison, larger average tumor size was measured in untreated mice ($1106.3 \pm 548.8 \text{ mm}^3$) (Fig. 3). The average tumor volume for mice receiving the scrambled sequence control vector, Ad-PD-L1ip3SC was similar to that of untreated mice ($1026.8 \pm 143.6 \text{ mm}^3$). In this experimental scheme, the inoculation of the CT26 tumor cells initiated the host antitumor immunity, while the effect of the PD-L1 blockade by the tumor-site production of PD-L1ip3 owing to Ad-PD-L1ip3 transduction or by treatment with PD-L1ip3 in peptide form was evaluated within 3 weeks after the tumor cell inoculation. We speculate that the host anti-tumor immunity against tumor cells was not sufficiently stimulated at this

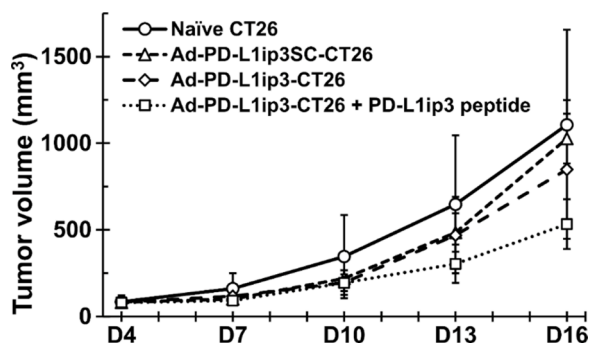


Fig. 3. Treatment with Ad-PD-L1ip3 transduction alone or in combination with PD-L1ip3 in peptide form attenuated the growth of subcutaneously inoculated CT26 cell tumors in the mouse. The vector carrying the scrambled peptide gene (AD-PD-L1ip3SC) did not show any significant tumor growth attenuation as compared to untreated CT26 cell tumors. Results are presented as mean \pm SD ($n = 5$).

time; therefore, the PD-L1 blockade therapy in this acute syngeneic murine model appeared to be inadequate. A longer exposure time to tumor antigens is suggested to be more appropriate for the adequate evaluation of the PD-L1 blockade therapy by either the tumor-site production of PD-L1ip3 or in combination with daily administration of PD-L1ip3 in peptide form.

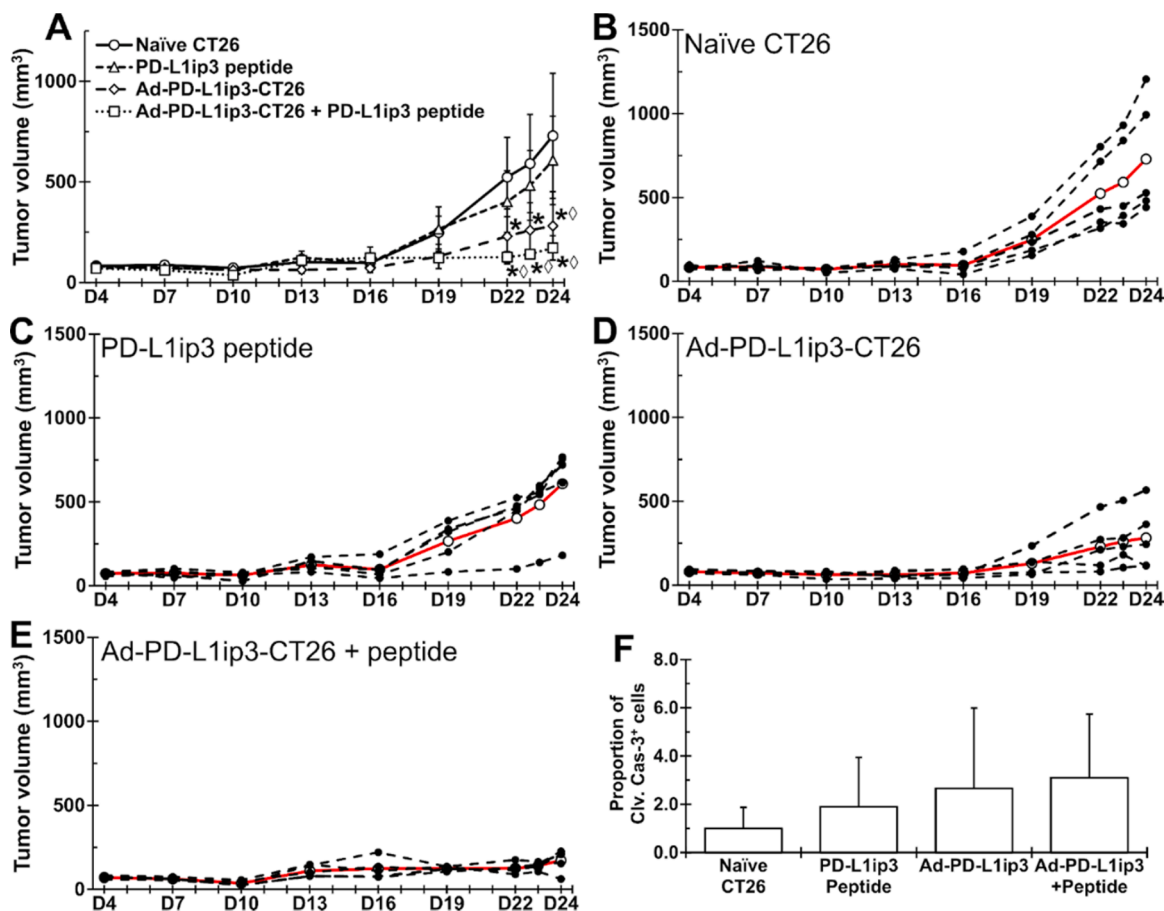


Fig. 4. Prior stimulation of host immunity by CT26 cell lysate enhanced the inhibitory effect of PD-L1ip3 and attenuated the growth of subcutaneously inoculated CT26 tumors in the mouse by apoptosis. (A–E) Panel A shows the average tumor size, while panels B–E show volumes of individual tumors in each treatment group. Red line in panels B–E indicates average tumor volume in each group. Results are presented as mean \pm SD ($n = 5–6$). *, $P < 0.05$ with Naïve CT26, \diamond , $P < 0.05$ with PD-L1ip3 peptide (F) Treatment with Ad-PD-L1ip3 transduction and combination with PD-L1ip3 peptide treatment increased apoptotic cells in CT26 tumors. Results are presented as mean \pm SD ($n = 5$).

Pretreatment with CT26 cell lysate enhanced inhibition of tumor growth by Ad-PD-L1ip3 and the combination treatment with the PD-L1ip3 peptide

We hypothesized that pretreatment with CT26 cell lysate might enhance the inhibition of CT26 tumor growth by Ad-PD-L1ip3 seen in the last section. To validate this hypothesis, mice were pre-treated with CT26 cell lysate before cancer cell inoculation, 3 times separated by 1-week intervals. As shown in Fig. 4A–E, Ad-PD-L1ip3 transduction into CT26 cells significantly attenuated the growth of the tumors ($281.4 \pm 169.6 \text{ mm}^3$, $P < 0.05$), and the tumor growth attenuation effect was further enhanced by the combination treatment including PD-L1ip3 in peptide form ($172.6 \pm 60.9 \text{ mm}^3$, $P < 0.05$) compared to the untreated CT26 cell tumors ($729.6 \pm 310.3 \text{ mm}^3$). On the other hand, treatment with only the peptide form of PD-L1ip3 showed a minimal effect on tumor growth ($607.5 \pm 220.1 \text{ mm}^3$). These results suggest that our PD-L1 blockade treatment combining adenoviral vector-based gene therapy along with direct administration of PD-L1ip3 in peptide form is effective in inhibiting tumor growth, presumably due to the blockade of PD-L1 and PD-1 immune checkpoint mechanism.

Treatment with PD-L1ip3 in peptide form and combination with gene transduction by Ad-PD-L1ip3 increased apoptotic cells in CT26 cell tumors in mice

As shown in Fig 2, PD-L1ip3 peptide increased the cell death of CT26 cells in the presence of antigen-primed CT26-T cell *in vitro*. Therefore,

changes in apoptotic cell numbers in tumor nodules were evaluated by immunohistochemistry. Immunohistochemical analysis of cleaved caspase-3 positive cells in tumor nodules suggested that both mono treatment with gene transduction by Ad-PD-L1ip3 and a combination treatment with Ad-PD-L1ip3 transduction and administration of PD-L1ip3 in peptide form increased apoptotic cell numbers in tumors as compared to PBS-treated mouse tumors (Fig. 4F). However, given the large data variation, no statistically significant difference between the groups was observed.

Discussion

Anticancer immunity plays an important role in the spontaneous inhibition of cancer growth [29,30]. The success of immunotherapy, which has been established in the last decade as a treatment against multiple immunogenic cancers, including non-small cell lung cancers and colorectal cancer [31–37], supports this notion. Therefore, the development of safer, less toxic, and more effective enhancers of anti-cancer immunity would be beneficial for both cancer patients as well as society at large. Currently, the most common strategy for cancer immunotherapy is the systemic administration of humanized antibodies against immune checkpoint proteins, such as CTLA-4 and PD-1. Although these antibody-based therapeutics for cancer immunotherapy exhibit solid efficacy against immunogenic cancers, their off-target effects due to an enhancement of host immunity remain problematic [38]. To address these problems, we sought to design a local immune therapy by focusing on the PD-L1 blockade within the tumor microenvironment using an adenovirus engineered to carry a PD-L1 inhibitory peptide gene.

To accomplish this purpose, we designed a novel peptide for inhibiting PD-L1 using a series of computational methods, followed by experimental validation. First, we generated several candidate PD-L1 inhibitory peptide sequences using the PinaColada algorithm and the x-ray structure of the PD-L1:PD-1 complex. These sequences were then screened by creating several candidate complexes with flexible molecular docking (with the peptide near the PD-L1:PD-1 binding interface) and then the binding affinity was estimated for each complex using molecular dynamics simulation (the MM-PBSA method). The two peptides with the highest estimated affinity for PD-L1 underwent further molecular dynamics simulations, which demonstrated the stability of complexes formed with the peptide denoted PD-L1ip3 on the sub-microsecond timescale. Experimental confirmation of the specific binding of this peptide to PD-L1 showed an affinity in the micromolar range. This unique peptide may have applications outside the scope of the present study and likely could be further optimized to obtain more potent PD-L1 inhibition.

The effect of the peptide (PD-L1ip3) on tumor growth was considered in three different ways: direct administration in peptide form, delivery of a secretory gene encoding the peptide by an adenovirus vector, and a combination of the two administration routes. These treatments were tested on a murine colon carcinoma cell line, which was evaluated in conventional cell culture and a co-culture with CT26 cell antigen-primed CD8⁺ T cells (CT26-T cells). As expected, neither direct administration of the PD-L1ip3 in peptide form nor gene transduction by the adenovirus vector altered cell growth in conventional cell culture (Fig. S2). However, PD-L1ip3 in peptide form, but not gene transduction by the adenovirus vector, significantly increased CT26-T cell-dependent death of colon carcinoma cells in co-culture (Fig. 2B). Cancer apoptosis induced by expression of the PD-L1ip3 gene showed a clear increase as compared to that by the PBS control (Fig. 2B) although its increase was much smaller than that by the direct peptide treatment and the statistical significance was not observed between the groups due to a relatively large variation in the gene transduction group. This result is reasonably explained by the lower concentration of the inhibitory peptide in the culture medium due to the expression of the PD-L1ip3 gene as compared to the direct addition of 10 μ M of the peptide. These cell

culture studies, therefore, suggest the capability of the treatment with PD-L1ip3 peptide to stimulate cytotoxic T cell-induced cell death in cancer cells.

The ability of PD-L1ip3 peptide to stimulate cancer cell antigen-primed CD8⁺ T cells to induce cell death in colon carcinoma cells in co-culture studies (Fig. 2B) compelled an *in vivo* test of the efficacy of both PD-L1ip3 in peptide form and transduction of its gene by the Ad-PD-L1ip3 vector. In the mouse study, the effects of two mouse immune conditions, PD-L1ip3 in peptide form alone, Ad-PD-L1ip3 gene therapy alone, and a combination treatment with both direct peptide administration and gene therapy were evaluated in a subcutaneous tumor mouse model with CT26 murine colon carcinoma cells. First, the effect of direct administration of PD-L1ip3 and/or its gene expression was evaluated using syngeneic immunocompetent mice. Fig. 3 shows that the growth of Ad-PD-L1ip3 transduced cancer cells was slower than that of un-transduced cells and this tumor growth attenuation became further pronounced by the daily direct administration of PD-L1ip3 beginning at day 7 for 13 days although tumor growth slowly continued. However, neither transduction of a scrambled sequence peptide gene by the adenovirus vector (Ad-PD-L1ip3SC) nor PD-L1ip3 in peptide form alone showed a statistically significant change in tumor growth as compared to the growth of the untreated CT26 cells. On the other hand, when mice were previously treated with CT26 cell lysate three times for two weeks, mimicking chronic tumor antigen exposure, growth of Ad-PD-L1ip3 transduced cancer cells were significantly slower than that of un-transduced cells and this tumor growth was almost completely inhibited by the co-treatment with daily administration of PD-L1ip3 in peptide form starting at day 7 for 13 days. As expected, a sole treatment consisting of gene transduction by Ad-PD-L1ip3SC, a vector encoding the scrambled sequence control peptide, revealed no significant change in tumor growth as compared to the untreated group. The tumor growth pattern for individual mice in each group (Figs. 4B–4E) indicates clear efficacy of co-treatment with the Ad-PD-L1ip3 vector and PD-L1ip3 in peptide form. These results demonstrate the possibility of tumor cell-targeted gene therapy with a PD-L1 inhibitory peptide gene along with direct peptide administration. Since the peptide showed no cytotoxicity (Fig. S2) and the activation of CD8⁺ T cells occurs presumably in tumor tissue, this method is considered to be a safe immune checkpoint therapy. However, understanding the fate of the PD-L1ip3-activated T cells and overall safety warrant further study.

The discrepancy between the relatively small effect of PD-L1ip3 gene expression on cancer cell death in the co-culture study (Fig. 2B) versus its considerable effect in the mouse study (Figs. 3 and 4) may be explained by the difference in the participating cell types and the duration of the study. The cell culture study included only two cell types, effector T cells and cancer cells, whereas other cell types including natural killer cells (NK cells) are potentially participating in cancer cell death during the mouse study [39–41]. Second, the T cell-induced death of cancer cells was monitored only 72 h after gene transduction by Ad-PD-L1ip3 in the co-culture study, whereas the tumor growth effect was monitored for two weeks in the mouse study. In support of the involvement of the PD-L1/PD-1 immune checkpoint mechanism in other immune cells. A recent report describes the importance of PD-1[−] NK cells in anti-cancer immunity for mouse cancer models [42] and human lung cancer [43]. Moreover, blockade of PD-L1⁺ NK cells by an anti-PD-L1 antibody is shown to increase therapeutic efficacy in human patients [44], suggesting that PD-L1 in NK cells is an inhibitory molecule in NK cell-induced oncolysis. Therefore, the determination of potential targets for this PD-L1 inhibitory peptide must be studied thoroughly.

Overall, the computationally designed peptide, PD-L1ip3, was demonstrated to bind to PD-L1 in experiment. Treatment with this peptide alone showed negligible cytotoxicity but stimulated cancer antigen-primed CD8⁺ T cells in an oncolysis assay. Transduction of the PD-L1ip3 gene by an adenovirus vector into CT26 colon carcinoma cells significantly attenuated tumor growth in mice when their immune systems were previously stimulated by CT26 cell lysate. Tumor growth of

PD-L1p3-expressing CT26 cells was almost completely inhibited by a combination treatment of direct administration of PD-L1p3 in peptide form along with an adenovirus gene therapy encoding the same peptide. Although further studies are required to confirm potential target immune cells and the safety of PD-L1p3 by orthodox pharmacokinetics, pharmacodynamics, multispecies toxicity studies, and comparative study with existing anti-PD-1/PD-L1 antibody therapy, the data presented here show that this peptide therapy could be a locally effective agent to stimulate antitumor immunity, thereby inhibiting colon cancer growth.

CRedit authorship contribution statement

Susumu Ishiguro: Data curation, Formal analysis, Investigation, Methodology, Validation, Visualization, Writing – original draft, Writing – review & editing. **Deepa Upreti:** Data curation, Formal analysis, Investigation, Methodology, Validation, Visualization, Writing – original draft, Writing – review & editing. **Molly Bassette:** Investigation, Methodology. **E.R. Azhagiya Singam:** Formal analysis, Investigation, Methodology, Software, Visualization. **Ravindra Thakkar:** Formal analysis, Investigation, Software, Visualization. **Mayme Loyd:** Investigation. **Makoto Inui:** Investigation, Methodology, Resources. **Jeffrey Comer:** Data curation, Formal analysis, Funding acquisition, Investigation, Methodology, Project administration, Resources, Software, Supervision, Validation, Visualization, Writing – review & editing. **Masaaki Tamura:** Conceptualization, Data curation, Funding acquisition, Investigation, Methodology, Project administration, Resources, Supervision, Validation, Writing – original draft, Writing – review & editing.

Declaration of Competing Interest

None.

Acknowledgments

We thank Drs. Jodi McGill (Veterinary Microbiology and Preventive Medicine, Iowa State University College of Veterinary Medicine) and Waithaka Mwangi for technical instruction for *in vitro* T cell assay. We thank Mr. Kaori Knights (Department of Diagnostic Medicine/Pathobiology, Kansas State University) for his technical support on the flow cytometer. We also thank Dr. Chieko Azuma and Mr. Randall Juracek (Department of Clinical Sciences, Kansas State University) for technical assistance during the irradiation of cancer cells.

Funding

This research was supported in part by [Kansas State University \(KSU\)](#) College of Veterinary Medicine Dean's funds [2015CVM-SMILE] (MT), KSU Johnson Cancer Research Center [2018 JCRC-IRA] (MT), K-INBRE Scholar Award [P20 GM103418] (MB) and National Cancer Institute [1 R15 CA219919-01] (MT, JC). This work was partially supported by the [National Science Foundation \(NSF\)](#) under award number DMR-1945589 (JC). A majority of the computing for this project was performed on the Beocat Research Cluster at Kansas State University, which is funded in part by NSF grant, CHE-1726332 (JC).

Supplementary materials

Supplementary material associated with this article can be found, in the online version, at [doi:10.1016/j.tranon.2021.101337](https://doi.org/10.1016/j.tranon.2021.101337).

References

- [1] R.L. Siegel, K.D. Miller, H.E. Fuchs, A. Jemal, Cancer statistics, 2021, *CA Cancer J. Clin.* 71 (2021) 7–33, <https://doi.org/10.3322/caac.21654>.
- [2] P. Peltomaki, Role of DNA mismatch repair defects in the pathogenesis of human cancer, *J. Clin. Oncol.* 21 (2003) 1174–1179, <https://doi.org/10.1200/JCO.2003.04.060>, official journal of the American Society of Clinical Oncology.
- [3] S. Emambux, G. Tachon, A. Junca, D. Tougeron, Results and challenges of immune checkpoint inhibitors in colorectal cancer, *Expert Opin. Biol. Ther.* 18 (2018) 561–573, <https://doi.org/10.1080/14712598.2018.1445222>.
- [4] A. Kalyan, S. Kircher, H. Shah, M. Mulcahy, A. Benson, Updates on immunotherapy for colorectal cancer, *J. Gastrointest. Oncol.* 9 (2018) 160–169, <https://doi.org/10.21037/jgo.2018.01.17>.
- [5] J.M. Michot, C. Bigenwald, S. Champiat, M. Collins, F. Carbonnel, S. Postel-Vinay, A. Berdelou, A. Varga, R. Bahleda, A. Hollebecque, C. Massard, A. Fuerea, V. Ribrag, A. Gazzah, J.P. Armand, N. Amellal, E. Angevin, N. Noel, C. Boutros, C. Mateus, C. Robert, J.C. Soria, A. Marabelle, O. Lambotte, Immune-related adverse events with immune checkpoint blockade: a comprehensive review, *Eur. J. Cancer* 54 (2016) 139–148, <https://doi.org/10.1016/j.ejca.2015.11.016>.
- [6] A. Ribas, J.D. Wolchok, Cancer immunotherapy using checkpoint blockade, *Science* 359 (2018) 1350–1355, <https://doi.org/10.1126/science.aar4060>.
- [7] P. Sharma, S. Hu-Lieskovan, J.A. Wargo, et al., Primary, adaptive, and acquired resistance to cancer immunotherapy, *Cell* 168 (2017) 707–723, <https://doi.org/10.1016/j.cell.2017.01.017>.
- [8] Z. Liu, R. Ravindranathan, P. Kalinski, Z.S. Guo, D.L. Bartlett, Rational combination of oncolytic vaccinia virus and PD-L1 blockade works synergistically to enhance therapeutic efficacy, *Nat. Commun.* 8 (2017) 14754, <https://doi.org/10.1038/ncomms14754>.
- [9] D.C. Mansfield, J.N. Kyula, N. Rosenfelder, J. Chao-Chu, G. Kramer-Marek, A. A. Khan, V. Roulstone, M. McLaughlin, A.A. Melcher, R.G. Vile, H.S. Pandha, V. Khoo, K.J. Harrington, Oncolytic vaccinia virus as a vector for therapeutic sodium iodide symporter gene therapy in prostate cancer, *Gene Ther.* 23 (2016) 357–368, <https://doi.org/10.1038/gt.2016.5>.
- [10] G. Marelli, A. Howells, N.R. Lemoine, Y. Wang, Oncolytic viral therapy and the immune system: a double-edged sword against cancer, *Front. Immunol.* 9 (2018) 866, <https://doi.org/10.3389/fimmu.2018.00866>.
- [11] Y. Zheng, Y.C. Fang, J. Li, PD-L1 expression levels on tumor cells affect their immunosuppressive activity, *Oncol. Lett.* 18 (2019) 5399–5407, <https://doi.org/10.3892/ol.2019.10903>.
- [12] M. Iwasaki, Y. Tanaka, H. Kobayashi, K. Murata-Hirai, H. Miyabe, T. Sugie, M. Toi, N. Minato, Expression and function of PD-1 in human gamma-delta T cells that recognize phosphoantigens, *Eur. J. Immunol.* 41 (2011) 345–355, <https://doi.org/10.1002/eji.201040959>.
- [13] K.E. Pauken, M. Dougan, N.R. Rose, A.H. Lichtman, A.H. Sharpe, Adverse events following cancer immunotherapy: obstacles and opportunities, *Trends Immunol.* 40 (2019) 511–523, <https://doi.org/10.1016/j.it.2019.04.002>.
- [14] D. Zaidman, H.J. Wolfson, PinaColada: peptide-inhibitor ant colony ad-hoc design algorithm, *Bioinformatics* 32 (2016) 2289–2296, <https://doi.org/10.1093/bioinformatics/btw133>.
- [15] K.M. Zak, R. Kitel, S. Przetocka, P. Golik, K. Guzik, B. Musielak, A. Domling, G. Dubin, T.A. Holak, Structure of the complex of human programmed death 1, PD-1, and its ligand PD-L1, *Structure* 23 (2015) 2341–2348, <https://doi.org/10.1016/j.str.2015.09.010>.
- [16] M. Kurcinski, M. Jamroz, M. Blaszczyk, A. Kolinski, S. Kmiecik, CABS-dock web server for the flexible docking of peptides to proteins without prior knowledge of the binding site, *Nucleic Acids Res.* 43 (2015) W419–W424, <https://doi.org/10.1093/nar/gkv456>.
- [17] R. Salomon-Ferrer, D.A. Case, R.C. Walker, An overview of the Amber biomolecular simulation package, *Wiley Interdiscip. Rev. Comput. Mol. Sci.* 3 (2013) 198–210.
- [18] H. Gouda, I.D. Kuntz, D.A. Case, P.A. Kollman, Free energy calculations for theophylline binding to an RNA aptamer: comparison of MM-PBSA and thermodynamic integration methods, *Biopolymers* 68 (2003) 16–34, <https://doi.org/10.1002/bip.10270>.
- [19] J.A. Maier, C. Martinez, K. Kasavajhala, L. Wickstrom, K.E. Hauser, C. Simmerling, ffl4SB: improving the Accuracy of Protein Side Chain and Backbone Parameters from ff99SB, *J. Chem. Theory Comput.* 11 (2015) 3696–3713, <https://doi.org/10.1021/acs.jctc.5b00255>.
- [20] T. Darden, D. York, L. Pedersen, Particle mesh Ewald: an N · log(N) method for Ewald sums in large systems, *J. Chem. Phys.* 98 (1993) 10089–10092.
- [21] S.E. Feller, Y. Zhang, R.W. Pastor, B.R. Brooks, Constant pressure molecular dynamics simulation: the Langevin piston method, *J. Chem. Phys.* 103 (1995) 4613–4621.
- [22] J.C. Phillips, R. Braun, W. Wang, J. Gumbart, E. Tajkhorshid, E. Villa, C. Chipot, R. D. Skeel, L. Kale, K. Schulten, Scalable molecular dynamics with NAMD, *J. Comput. Chem.* 26 (2005) 1781–1802, <https://doi.org/10.1002/jcc.20289>.
- [23] S. Ishiguro, D. Uppalapati, Z. Goldsmith, D. Robertson, J. Hodge, H. Holt, A. Nakashima, K. Turner, M. Tamura, Exopolysaccharides extracted from *Parachlorella kessleri* inhibit colon carcinoma growth in mice via stimulation of host antitumor immune responses, *PLoS ONE* 12 (2017), e0175064, <https://doi.org/10.1371/journal.pone.0175064>.
- [24] C. Doi, D.K. Maurya, M.M. Pyle, D. Troyer, M. Tamura, Cytotherapy with naive rat umbilical cord matrix stem cells significantly attenuates growth of murine pancreatic cancer cells and increases survival in syngeneic mice, *Cytotherapy* 12 (2010) 408–417, <https://doi.org/10.3109/14653240903548194>.
- [25] S. Ishiguro, K. Yoshimura, R. Tsunedomi, M. Oka, S. Takao, M. Inui, A. Kawabata, T. Wall, V. Magafa, P. Cordopatis, A.G. Tzakos, M. Tamura, Involvement of angiotensin II type 2 receptor (AT2R) signaling in human pancreatic ductal adenocarcinoma (PDAC): a novel AT2R agonist effectively attenuates growth of

- PDAC grafts in mice, *Cancer Biol. Ther.* 16 (2015) 307–316, <https://doi.org/10.1080/15384047.2014.1002357>.
- [26] R. Magnez, B. Thiroux, S. Taront, Z. Segaula, B. Quesnel, X. Thuru, PD-1/PD-L1 binding studies using microscale thermophoresis, *Sci. Rep.* 7 (2017) 17623, <https://doi.org/10.1038/s41598-017-17963-1>.
- [27] X. Cheng, V. Veverka, A. Radhakrishnan, L.C. Waters, F.W. Muskett, S.H. Morgan, J. Huo, C. Yu, E.J. Evans, A.J. Leslie, M. Griffiths, C. Stubberfield, R. Griffin, A. J. Henry, A. Jansson, J.E. Ladbury, S. Ikemizu, M.D. Carr, S.J. Davis, Structure and interactions of the human programmed cell death 1 receptor, *J. Biol. Chem.* 288 (2013) 11771–11785, <https://doi.org/10.1074/jbc.M112.448126>.
- [28] Y. Iwai, M. Ishida, Y. Tanaka, T. Okazaki, T. Honjo, N. Minato, Involvement of PD-L1 on tumor cells in the escape from host immune system and tumor immunotherapy by PD-L1 blockade, *Proc. Natl. Acad. Sci. U. S. A.* 99 (2002) 12293–12297, <https://doi.org/10.1073/pnas.192461099>.
- [29] J.A. Thomas, M. Badini, The role of innate immunity in spontaneous regression of cancer, *Indian J. Cancer* 48 (2011) 246–251, <https://doi.org/10.4103/0019-509X.82887>.
- [30] T. Jessy, Immunity over inability: the spontaneous regression of cancer, *J. Nat. Sci. Biol. Med.* 2 (2011) 43–49, <https://doi.org/10.4103/0976-9668.82318>.
- [31] N.A. Johdi, N.F. Sukor, Colorectal Cancer Immunotherapy: options and Strategies, *Front. Immunol.* 11 (2020) 1624, <https://doi.org/10.3389/fimmu.2020.01624>.
- [32] G. Golshani, Y. Zhang, Advances in immunotherapy for colorectal cancer: a review, *Ther. Adv. Gastroenterol.* 13 (2020), 1756284820917527, <https://doi.org/10.1177/1756284820917527>.
- [33] V. Vanella, L. Festino, M. Strudel, E. Simeone, A.M. Grimaldi, P.A. Ascierto, PD-L1 inhibitors in the pipeline: promise and progress, *Oncoimmunology* 7 (2017), e1365209, <https://doi.org/10.1080/2162402X.2017.1365209>.
- [34] A.P. Silva, P.V. Coelho, M. Anazetti, P.U. Simioni, Targeted therapies for the treatment of non-small-cell lung cancer: monoclonal antibodies and biological inhibitors, *Hum. Vaccin Immunother.* 13 (2017) 843–853, <https://doi.org/10.1080/21645515.2016.1249551>.
- [35] L. Chen, X. Han, Anti-PD-1/PD-L1 therapy of human cancer: past, present, and future, *J. Clin. Invest.* 125 (2015) 3384–3391, <https://doi.org/10.1172/JCI80011>.
- [36] M. Wang, B. Yin, H.Y. Wang, R.F. Wang, Current advances in T-cell-based cancer immunotherapy, *Immunotherapy* 6 (2014) 1265–1278, <https://doi.org/10.2217/imt.14.86>.
- [37] C. Kyi, M.A. Postow, Checkpoint blocking antibodies in cancer immunotherapy, *FEBS Lett.* 588 (2014) 368–376, <https://doi.org/10.1016/j.febslet.2013.10.015>.
- [38] D. Day, A.R. Hansen, Immune-related adverse events associated with immune checkpoint inhibitors, *BioDrugs: clinical immunotherapeutics, biopharmaceuticals and gene therapy*, 30 (2016) 571–584, 10.1007/s40259-016-0204-3.
- [39] M. Vogler, S. Shanmugalingam, V. Sarchen, L.M. Reindl, V. Greze, L. Buchinger, M. Kuhn, E. Ullrich, Unleashing the power of NK cells in anticancer immunotherapy, *J. Mol. Med.* (2021), <https://doi.org/10.1007/s00109-021-02120-z>.
- [40] C. Zhang, Y. Hu, C. Shi, Targeting natural killer cells for tumor immunotherapy, *Front. Immunol.* 11 (2020) 60, <https://doi.org/10.3389/fimmu.2020.00060>.
- [41] P. Minetto, F. Guolo, S. Pesce, M. Greppi, V. Obino, E. Ferretti, S. Sivori, C. Genova, R.M. Lemoli, E. Marcenaro, Harnessing NK cells for cancer treatment, *Front. Immunol.* 10 (2019) 2836, <https://doi.org/10.3389/fimmu.2019.02836>.
- [42] J. Hsu, J.J. Hodgins, M. Marathe, C.J. Nicolai, M.C. Bourgeois-Daigneault, T. N. Trevino, C.S. Azimi, A.K. Scheer, H.E. Randolph, T.W. Thompson, L. Zhang, A. Iannello, N. Mathur, K.E. Jardine, G.A. Kirn, J.C. Bell, M.W. McBurney, D. H. Raulet, M. Ardolino, Contribution of NK cells to immunotherapy mediated by PD-1/PD-L1 blockade, *J. Clin. Invest.* 128 (2018) 4654–4668, <https://doi.org/10.1172/JCI99317>.
- [43] C. Niu, M. Li, S. Zhu, Y. Chen, L. Zhou, D. Xu, J. Xu, Z. Li, W. Li, J. Cui, PD-1-positive Natural Killer Cells have a weaker antitumor function than that of PD-1-negative Natural Killer Cells in Lung Cancer, *Int. J. Med. Sci.* 17 (2020) 1964–1973, <https://doi.org/10.7150/ijms.47701>.
- [44] W. Dong, X. Wu, S. Ma, Y. Wang, A.P. Nalin, Z. Zhu, J. Zhang, D.M. Benson, K. He, M.A. Caligiuri, J. Yu, The mechanism of anti-PD-L1 antibody efficacy against PD-L1-negative tumors identifies NK cells expressing PD-L1 as a cytolytic effector, *Cancer Discov.* 9 (2019) 1422–1437, <https://doi.org/10.1158/2159-8290.CD-18-1259>.